

Throughput of the Magnetic Induction Based Wireless Underground Sensor Networks: Key Optimization Techniques

Steven Kisseleff, *Student Member, IEEE*, Ian F. Akyildiz, *Fellow, IEEE*, and Wolfgang H. Gerstaecker, *Senior Member, IEEE*

Abstract—Wireless underground sensor networks (WUSNs) present a variety of new research challenges. Recently, a magnetoinductive (MI) waveguide technique has been proposed to cope with the very harsh propagation conditions in WUSNs. This relay-based approach allows for an extension of the transmission range, which can be quite limited if relays are not deployed. In this paper, tree-based WUSNs are considered. The objective of our work is to determine the optimal system parameters, topology, and deployment strategy in order to avoid bottlenecks in the system and achieve optimal network throughput. We compare two different deployment schemes: MI waveguides and direct MI transmission (no relays deployed) based connections between sensors. The two schemes are different in nature and propagation characteristics. Therefore, different optimization techniques are utilized. The optimal set of system parameters is chosen to maximize the channel capacity of the worst link and therefore optimize the available data rate. The bottleneck throughput of the direct MI transmission based network can be then compared with the respective results of the MI waveguides based network. In several cases, we observe a better performance of the direct MI transmission based networks.

Index Terms—Magnetic induction based transmission, throughput optimization, wireless underground sensor networks.

I. INTRODUCTION

THE recent research on Wireless Underground Sensor Networks (WUSNs) is mainly focused on establishing an efficient wireless communication in the underground medium. Since the propagation medium consists of soil, rock, and sand, traditional wireless signal propagation techniques using electromagnetic (EM) waves can be only applied for very small transmission ranges due to the high path loss and vulnerability to changes of soil properties, such as moisture [3]. Typical ap-

plications of these networks include soil condition monitoring, earthquake prediction, border patrol, etc., [4], [5].

Magnetic induction (MI) communication has been studied in various works, mostly in context of the near-field communication (NFC) and wireless power transfer [6]–[9]. These works provide some insight into the design aspects for point-to-point MI based signal transmissions.

MI based WUSNs were first introduced in [5] and make use of magnetic antennas implemented as coils, which are combined in waveguide structures with several passive relay devices between two transceiver nodes according to [10]–[13]. Similar to traditional wireless relaying concepts, the MI solution benefits from a lower equivalent path loss. Consequently, the transmission range can be greatly improved compared to the EM waves based approach for WUSNs [5].

The network throughput, also called network capacity, was intensively studied for different network paradigms in the past [14]–[17] including magnetic induction based WUSNs in [18] where a scaling law is provided by adopting a channel model from [10]. One of the assumptions in [10] is a weak coupling between the coils in an MI waveguide, independent of the system parameters. However, as it was shown in [19], for an MI waveguide with high relay density, the MI is very large and the system parameters can be adjusted to maximize the channel capacity for a given waveguide. Further differences to the traditional wireless networks are interference propagation and variations of the channel and noise characteristics depending on the topology of the network, which have been not considered in [10]. This leads to a significant difference in channel models and in network design.

The polarization of the EM waves is a well-known dimension which can be exploited to improve the system performance in terms of signal-to-interference-plus-noise-ratio (SINR), diversity, and throughput [20]–[22]. In this work, we apply the polarization to the coils, which we model as dipoles. The polarization is used to avoid or reduce the interfering signals, which cause a degradation of the SINR, such that in certain slots no reasonable transmission can be accomplished.

As it was discussed in [19], [23], and [7], the channel capacity of an MI based link depends on the choice of the system parameters, like the size of the coils, resonance frequency f_0 , and number of coil windings N . A practical sensor network may contain various links with different numbers of relays and therefore the optimal parameters may differ from link to link.

Manuscript received March 4, 2014; revised July 17, 2014 and October 24, 2014; accepted October 26, 2014. Date of publication November 4, 2014; date of current version December 15, 2014. This work was supported by the German Research Foundation (Deutsche Forschungsgemeinschaft, DFG) under Grant GE 861/4-1. This paper was presented in part at the IEEE PIMRC 2013 and IEEE GLOBECOM 2013. The associate editor coordinating the review of this paper and approving it for publication was R. Dinis.

S. Kisseleff and W. H. Gerstaecker are with the Institute for Digital Communications, Friedrich-Alexander-University Erlangen-Nürnberg (FAU), 91058 Erlangen, Germany (e-mail: kisseleff@LNT.de; gersta@LNT.de).

I. F. Akyildiz is with the School of Electrical and Computer Engineering, Georgia Institute of Technology, Atlanta, GA 30308 USA (e-mail: ian@ece.gatech.edu).

Color versions of one or more of the figures in this paper are available online at <http://ieeexplore.ieee.org>.

Digital Object Identifier 10.1109/TCOMM.2014.2367030

In order to overcome the problems of individual manufacturing of each sensor node and implementing additional coils for multiple connected waveguides, one of our objectives in this work is the unification of the system parameters, which will result from an optimization problem. Hence, we assume that all devices are equipped with the same set of passive and active elements. In addition, a practical multinode network differs from a single waveguide connection, which is optimized in [19], in its signal propagation characteristics and interference coming from other nodes transmitting simultaneously. These interfering signals cannot be avoided via frequency-division multiple access (FDMA) by allocating a unique resonance frequency to each device, because all nodes transmit at the same resonance frequency due to the parameter unification. Furthermore, assuming that a common resonance frequency is used by all sensor nodes, an FDMA scheme cannot be established by subdividing the total transmission band in sub-bands due to a very narrow low path loss region around the resonance frequency, such that most of the sub-bands cannot be used for transmission. In addition, code-division multiple access (CDMA) is not reasonable due to the much higher bandwidth required for spreading. Therefore, we assume a time-division multiple access (TDMA) scheme, such that high power interference signals can be avoided. This yields a routing optimization problem and extends the original approach towards the optimization of the network throughput. The synchronization of transmissions for TDMA can be done using the well known approaches in [24].

In this paper, we focus on tree-based networks with a single sink, which collects the data from all nodes. The sink can be implemented as a node, which is connected wirelessly or via wireline with a mobile or removable aboveground device. This network structure is appropriate for most of the target applications with the primary goal of data collection. Each node transmits not only its own information, but also relays all received data from other nodes. For this, we utilize the decode-and-forward relaying concept in this work. Also, we assume that no bit errors occur at the output of the decoder of each transceiver, i.e., transmission operates at channel capacity.

According to [14] and [18], the traffic load of a link equals the throughput of an information stream multiplied by the number of streams (routes) to be served by the node. This holds since in sensor networks it is frequently assumed that the data rates of all streams are equal. In order to avoid a loss of data packets, the traffic load has to be less or equal to the available data rate at the node corresponding to the channel capacity. However, the transmission may be disturbed by interfering signals coming from other nodes. Hence, a multinode scheduling needs to be established, thus reducing the data rate. The transceivers are operated in half-duplex mode. The signal reception and transmission is carried out in different time slots by means of TDMA.

The throughput optimization techniques for direct MI transmission (with no relays) based and MI waveguides based WUSNs have been investigated in [1] and [2], respectively. Due to a significant difference in nature and properties of the signal propagation of the two approaches (as pointed out in [19]), it is not possible to provide a global solution valid for both schemes. In addition, the deployment costs for MI waveguides based

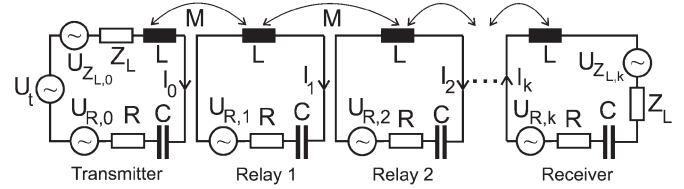


Fig. 1. Block diagram of MI waveguide with transmitter, receiver, and $(k - 1)$ relays.

networks are very high compared to the direct MI transmission based networks due to the increased number of coils. Hence, it is essential not only to ensure that the throughput of the network is optimized, but also that the deployment of the relays is beneficial. In this work, we compare the optimized network throughput of the two different schemes for given positions of sensor nodes, thus providing a fair comparison and a decision, which scheme should be favored under certain circumstances.

The first part of our contribution lies in the proposed new channel, noise, and interference models for MI based networks, which extend the existing point-to-point MI transmission models described in [19].¹ For this, we investigate the signal reflections in MI based networks. Secondly, we describe and apply novel approaches for throughput maximization. Here, the system parameters, network topology, and coil orientations are jointly optimized, in order to avoid the interference from the simultaneously transmitting signal sources and to reduce the path loss between connected sensor nodes, especially for the transmission link with the lowest throughput (bottleneck link).

This paper is organized as follows. In Section II, the system model is presented and the network structures are specified. In Section III, the problem of throughput maximization is formulated and the key optimization techniques for direct MI transmission based and MI waveguides based WUSNs, respectively, are presented. Section IV provides simulation results, especially a comparison between the two deployment approaches. Section V concludes the paper.

II. SYSTEM MODEL

Similar to [10], we assume that the waveguide structure comprises one transmitter circuit with a voltage source U_t , one receiver circuit with a load impedance Z_L , and $(k - 1)$ passive relays, which are placed equidistantly between the transceivers. Each circuit includes a magnetic antenna (which in this work is assumed to be a multilayer air core coil), a capacitor with capacitance C , and a resistor with resistance R (which models the copper resistance of the coil), see Fig. 1. Here, we do not consider parasitic effects (skin effect in windings, proximity effect, parasitic capacities), which may occur in circuit elements at very high frequencies. We assume that in the considered frequency ranges the influence of these effects is negligible which seems to be well justified. Because all involved signal mappings are linear for magnetic induction based transmissions, a linear

¹Note that [19] provides a theoretical point-to-point system model for MI based transmissions, which can be extended to a networked case due to its generality including the frequency selectivity of the path loss and noise.

channel model results. The inductivity of a multilayer air core coil is given by [25], [26]

$$L = \frac{21\mu N^2 a}{4\pi} \left(\frac{a}{l+h} \right)^{0.5}, \quad (1)$$

where N denotes the number of windings, a is the radius of the coil, $l = 0.5a$ is the length of the coil [25], h is the height of the windings over the coil surface, and μ denotes the permeability of the soil. The capacitance of the capacitor is chosen to make each circuit resonant at frequency f_0 [10], i.e., $C = \frac{1}{(2\pi f_0)^2 L}$. The copper resistance of the coil is given by [25]

$$R = \rho \cdot \frac{l_w}{A_w} = \rho \cdot \frac{2aN}{r_w^2}, \quad (2)$$

where $\rho \approx 1.678 \cdot 10^{-2} \Omega \cdot \text{mm}^2/\text{m}$ is the copper resistivity, l_w denotes the total wire length, A_w is the cross-section area of the wire, and r_w is the radius of the wire. The induced voltage is related to the coupling between the coils, which is determined by the mutual inductance [18]

$$M = \mu\pi N^2 \frac{a^4}{4r^3} \cdot J \cdot G, \quad (3)$$

where r denotes the distance between two considered coils. G is an additional loss factor due to eddy currents, as mentioned in [27]. The effect of eddy currents is explained in [28]. It yields an exponential decrease of the field strength with the transmission distance similar to the skin effect in copper wires. Hence, the loss factor G can be expressed as [19]

$$G = \exp\left(-\frac{r}{\delta}\right) \quad (4)$$

where δ is the skin depth, which depends on the signal frequency, conductivity and permittivity of soil [29]. We assume that these environmental parameters are known to the system designer. Of course, in case of sudden rainfalls or disasters the system may need to adapt to the time-varying channel conditions, but this issue is beyond the scope of this work.

Furthermore, in (3), J is the polarization factor. Note, that the well-known polarization factor [18]

$$J_{2D} = 2 \sin(\theta_t) \sin(\theta_r) + \cos(\theta_t) \cos(\theta_r) \quad (5)$$

is only valid in the two-dimensional space and therefore not fully applicable in our analysis. For the polarization factor in three-dimensional space, we obtain [1]

$$J = J_{3D} = 2 \sin(\theta_t) \sin(\theta_r) + \cos(\theta_t) \cos(\theta_r) \cos(\phi), \quad (6)$$

where θ_t and θ_r are the angles between the coil radial directions of transmitter and receiver, and the line connecting the two coil centers, respectively. ϕ is the angle difference in the plane orthogonal to the direction of transmission, see Fig. 2. Given the positions of transmitter and receiver coils and their axes orientation, the corresponding values for θ_t , θ_r , and ϕ can be determined using vector algebra.

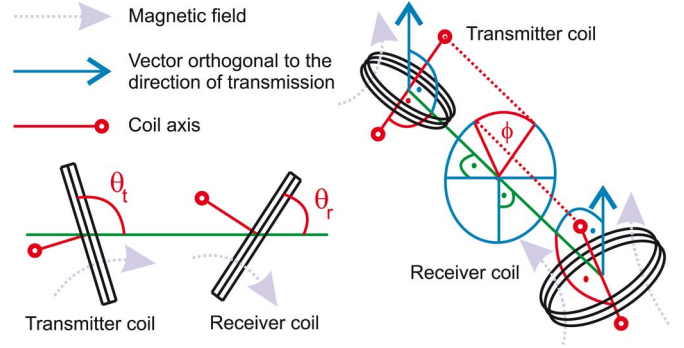


Fig. 2. Coil rotation and polarization angles.

A. Channel, Noise, and Interference Models of MI Based Links

For our investigations, we extend the channel and noise models for point-to-point transmissions proposed in [19]. These models enable a precise calculation of the signals arriving at the receiver, including noise, useful signal, and interference. For our mathematical analysis, we adopt the well-known function $S(x, x_L, k)$ as defined in [19]:

$$S(x, x_L, k) = F(x, k) + x_L \cdot F(x, k-1), \quad (7)$$

$$F(x, k) = x \cdot F(x, k-1) - F(x, k-2), \quad n \geq 2 \quad (8)$$

$$F(x, 0) = 1, \quad F(x, 1) = x, \quad (9)$$

where $x_L = \frac{R}{j2\pi fM}$ and $x = \frac{R+j2\pi fL + \frac{1}{j2\pi fC}}{j2\pi fM}$. From the difference equation (8), (9), a closed-form solution for $F(x, n)$ can be obtained as

$$F(x, n) = \frac{\left(\frac{(x+\sqrt{x^2-4})}{2}\right)^{n+1} - \left(\frac{(x-\sqrt{x^2-4})}{2}\right)^{n+1}}{\sqrt{x^2-4}}. \quad (10)$$

This function can be utilized in order to simplify the expressions for the path loss of the useful signal and the noise power at the receiver, where the noise stems from all resistors of the network and therefore has been propagated through the links along with the data signals. The amount of information, which can be transmitted error-free over the transmission link i is bounded by the Shannon channel capacity

$$C_{ch,i} = \int_{-\infty}^{+\infty} \log_2 \left(1 + \frac{P_{t,i}(f)}{L_{p,i}(f)P_{\text{disturb},i}(f)} \right) df, \quad (11)$$

where $P_{\text{disturb},i}(f) = P_{N,i}(f) + \sum_{j \neq i} P_{I,i,j}(f)$. $P_{\text{disturb},i}(f)$ is the average power spectral density of the disturbance of the signal, including the total average noise power spectral density $P_{N,i}(f)$ at the receiver of link i and the interference contribution $\sum_{j \neq i} P_{I,i,j}(f)$, where $P_{I,i,j}(f)$ is the interference power spectral density due to the j th interferer. $L_{p,i}(f)$ stands for the frequency-selective path loss, i.e., the frequency-dependent ratio of transmit and receive power. $P_{t,i}(f)$ represents the transmit power spectral density for link i and can be found via water filling (as shown in [19]) with the constraint of a total transmit power P , cf. [30]. For the calculation of the water filling solution, the channel state information is assumed to be

perfectly known to the system designer, since it only depends on the assumed environmental and system parameters.

Due to the stronger coupling between the transmission links in MI waveguides based networks, the calculation of the path loss, noise, and interference power spectral density differs from the straightforward calculation for a single link in [19] and [1]. Therefore, we show the derivation for both schemes (direct MI transmission and MI waveguides) separately.

1) *Direct MI Transmission Based Links*: The path loss of the link $L_{p,i}(f)$ can be calculated according to [19] by taking into account the additional load impedance in the receiver,

$$L_{p,i}(f) = \frac{|(x_i + x_{L,i}) [(x_i + x_{L,i})^2 - 1]|}{|\text{Im}\{x_{L,i}\}|}. \quad (12)$$

This path loss function describes all relevant signal propagation effects including attenuation, signal reflections and frequency splitting in MI based communication channels. The frequency splitting is, however, a minor issue in our scenario due to very weak couplings between coils in direct MI based transmissions, such that the two modes of the path loss function merge into one, as known from the literature [31]. Similarly, the additional signal reflections from the sensor nodes, which are not linked to the receiver of interest, can be neglected due to a much longer transmission route of these reflected signals and therefore a dramatically higher attenuation.

Based on the (12), we can determine the optimal load impedance Z_L for the direct MI transmission, such that the path loss $L_{p,i}(f_0)$ at the resonance frequency f_0 is minimized.

First we simplify (12) as

$$L_{p,i}(f_0) \approx \frac{|x_i + x_{L,i}|^3}{|x_{L,i}|} \Big|_{f=f_0} = \frac{(R + Z_L)^3}{Z_L |j2\pi f_0 M|^2}. \quad (13)$$

This function has a global minimum at $Z_L = R/2$. As discussed in [19], we assume the ambient noise due to EM waves to be negligible compared to the thermal noise produced in the copper resistors of the coils. The noise sources in the circuits of the surrounding devices including the transmitter can be neglected in direct MI transmission based WUSNs due to a high path loss [1], such that only the noise produced in the receiver circuit needs to be taken into account. This thermal noise is related to the resistances R and Z_L , see Fig. 1 ($k = 1$), yielding

$$P_{N,i}(f) \approx \frac{1}{2} \frac{4K_B T_K (R + Z_L) Z_L}{\left| R + j2\pi f L + \frac{1}{j2\pi f C} + Z_L \right|^2}, \quad (14)$$

where $K_B \approx 1.38 \cdot 10^{-23}$ J/K is the Boltzmann constant and T_K is the temperature in Kelvin.

For the further analysis the received interference power spectral density coming from other sensor nodes is required, which can be expressed as

$$P_{I,i,j}(f) = \frac{P_{t,I,i,j}(f)}{L_{p,I,j}(f)}, \quad (15)$$

where $P_{t,I,i,j}(f)$ is the transmit power spectral density of the interference source j and $L_{p,I,j}(f)$ is the path loss of the interfering signal from this source to the target receiver like in

(12). In a practical system, the transmit power spectral density is chosen to maximize the channel capacity of the connected link by applying the water filling algorithm (this choice is still valid for the useful signal in this work as mentioned before). However, in order to guarantee a certain available data rate, we assume a scenario, which can be considered as close to the worst case, where $P_{t,I,i,j}(f)$ maximizes the interference power similar to [2]:

$$P_{t,I,i,j}(f) = \frac{1}{L_{p,I,j}(f)} \cdot \frac{P}{\int_{-\infty}^{+\infty} \frac{1}{L_{p,I,j}(f)} df}, \quad (16)$$

where P is a total transmit power of each sensor node.

2) *MI Waveguides for WUSNs*: The recently proposed single MI waveguide system model according to [19] provides a good characterization of the behavior of a single link adopting an MI waveguide. However, the channel and noise models of connected MI waveguides in a network need to be further investigated, because they may differ significantly from the channel and noise models of a single MI waveguide. Due to many possible connections to every node, the path loss of the transmission becomes too complicated for an exact derivation. Therefore, we modify the existing channel and noise models of a single MI waveguide. For the transmitted signal, we assume that the receiver node is disconnected, such that no signal is reflected from the MI waveguides connected to the receiver node. This simplification is meaningful, because the influence from relays beyond the receiver node is very limited due to a high path loss, especially after a node circuit with a matched impedance. However, the path loss function in [19] needs to be changed accordingly, because due to the unification of the circuit elements the transmitter node circuit has additional load impedance, like the receiver node circuit. Starting with the voltage equation in the transmitter circuit and ignoring those interwaveguide reflections, which guide the transmitted signals back to the transmitter, we obtain for link i

$$U_{t,i} = (Z + Z_L) \cdot I_{t,i} - j2\pi f M_i \cdot I_{1,i} \cdot N_{c,i}, \quad (17)$$

where $I_{t,i}$ is the current in the transmitter, $I_{1,i}$ is the current in the first relay, $Z = R + j2\pi f L + \frac{1}{j2\pi f C}$, M_i is the mutual inductance related to the link i , and $N_{c,i}$ is the number of MI waveguides connected to the transmitter node. We exploit the fact that the induced current in the first relay coils is influenced by the magnetic field from the transmitter in a much stronger manner than by the relays close to the receiver due to the propagation distance. This assumption can be, however, violated by the network polarization described in Section III-C, where the coupling between coils of any two waveguides becomes different according to the waveguides' orientation. Then, it can be shown that the resulting path loss reduces, which results in an increased data rate. However, this effect is insignificant, because J from (6) ranges between 1 and 2 in our optimization.² Therefore, we assume that all coils have the same orientation, such that the induced currents in the first

²For the optimization of MI waveguides based WUSNs, we assume that all coils are rotated in the same direction. Thus, $1 \leq J \leq 2$ results from (6).

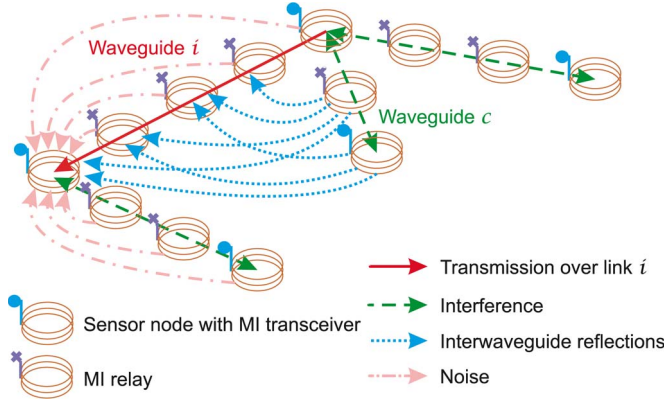


Fig. 3. Example of an MI waveguides based network illustrating different types of signals.

relays are similar for all waveguides connected to the same transmitter, yielding equal induced voltage in the transmitter coil. With the results from [19] and (17), we obtain

$$I_{k_i} = \frac{U_{t,i}}{j2\pi f M_i} \cdot \frac{1}{Q_i},$$

$$Q_i = (x_i + x_{L,i}) \cdot S(x_i, x_{L,i}, k_i) - N_{c,i} \cdot S(x_i, x_{L,i}, k_i - 1), \quad (18)$$

where $x_i = \frac{Z}{j2\pi f M_i}$ and $x_{L,i} = \frac{Z_L}{j2\pi f M_i}$. I_{k_i} is the current of the k_i th coil (receiver coil of the waveguide consisting of $k_i + 1$ coils) after transmitter i . In addition to this direct signal propagation, there are signal reflections from the waveguides connected to the same transmitter (interwaveguide reflections). These reflected signals are more attenuated due to a longer transmission route. We focus on the strongest signal reflections resulting from each of the connected waveguides c . According to this, every relay coil n_c of waveguide c with the length k_c influences every coil n_i of the target waveguide i with $n_i \geq n_c$, see Fig. 3. It can be shown that any other interwaveguide reflected signals ($n_i < n_c$) arriving at the receiver can be neglected due to an at least 15–20 dB higher path loss, since the total propagation route for these signals is dramatically longer. We denote $M'_{n_i, n_c, c}$ as mutual inductance between the relay n_i in the considered waveguide and relay n_c in the neighboring interfering waveguide c . Furthermore, we introduce a factor $x_i^{n_i - n_c}$ in order to compensate for less hops in the signal transmission route of the reflected signal than in the waveguide i , since the transfer function within the waveguide i can be given by $\approx \frac{1}{x_i}$ per hop, and a factor $\frac{1}{x'_{n_i, n_c, c}}$ with $x'_{n_i, n_c, c} = \frac{Z}{j2\pi f M'_{n_i, n_c, c}}$ for the hop from waveguide c to waveguide i . In particular, if $n_i - n_c = 1$ holds, the number of hops within the route of the reflected signal is equal to the number of hops in the waveguide i . Hence, the only difference between the interwaveguide reflected signal and the direct signal propagation for this case is due to a longer transmission distance for one of the hops (modeled by $\frac{1}{x'_{n_i, n_c, c}}$) than for any hop of the waveguide i (modeled by $\approx \frac{1}{x_i}$). Therefore, $I_{k_i, \text{refl}, n_i, n_c, c} =$

$\frac{U_{t,i}}{j2\pi f M_i} \frac{x_i}{Q_i} \frac{x_i}{x'_{n_i, n_c, c}}$ results³ with $\frac{x_i}{x'_{n_i, n_c, c}} \ll 1$. In general, the current induced from the reflected signals associated to waveguide c and coils n_c and n_i at the receiver k_i of link i is then approximately given by

$$I_{k_i, \text{refl}, n_i, n_c, c} = \frac{U_{t,i}}{j2\pi f M_i} \frac{x_i^{n_i - n_c}}{Q_i x'_{n_i, n_c, c}}. \quad (19)$$

The current from all significant reflected signals is

$$I_{k_i, \text{refl}} = \frac{U_{t,i}}{j2\pi f M_i} \frac{1}{Q_i} \sum_{c=1}^{N_{c,i}-1} \sum_{n_i=1}^{k_i} \sum_{n_c=1}^{\min(n_i, k_c)} \frac{x_i^{n_i - n_c}}{x'_{n_i, n_c, c}}, \quad (20)$$

where the number of interfering waveguides that have to be accounted for per link is equal to $N_{c,i} - 1$. This results in $I_{k_i, \text{total}} = I_{k_i} + I_{k_i, \text{refl}}$, and the path loss can be calculated as (cf. derivations for a single waveguide in [19])

$$L_{p,i}(f) = \frac{|S(x_i, x_{L,i}, k_i) Q_i|}{|\text{Im}\{x_{L,i}\}|} \times \left| 1 + \sum_{c=1}^{N_{c,i}-1} \sum_{n_i=1}^{k_i} \sum_{n_c=1}^{\min(n_i, k_c)} \frac{x_i^{n_i - n_c}}{x'_{n_i, n_c, c}} \right| \quad (21)$$

In principle, there is an infinite number of interwaveguide reflections, but with this procedure we take into account the strongest ones, which is sufficient for an accurate system analysis. Because our objective is a network design with identical devices, the load impedances in all nodes' circuits are identical and therefore not exactly matched to the waveguides, which may vary in their lengths. The optimal system parameters for the network may differ from the optimal parameters for a particular single waveguide, which leads to a decrease in magnetic induction, such that the approximation $F(x, k) \approx x^k$ holds and the matched impedance can be given by $Z_L = \text{Re}\{j2\pi f_0 M_i \cdot \frac{F(x_0, k+1)}{F(x_0, k)}\} \approx R$ with $x_0 = x(f = f_0)$, cf. [19].

Due to the increased number of coils in a network, the noise power at the receiver is significantly greater than that for a single waveguide transmission. We focus on the thermal noise produced in the waveguides according to Fig. 3, which are directly connected to the receiver of interest, since these are the dominant contributions taking into account the high path loss of transmission. Except for the noise produced by the load impedance in the receiver circuit, we approximate the noise power densities of all MI waveguides connected to one receiver node by the sum of the noise power densities produced by these waveguides (including waveguide i), when each of them is solely connected to the receiver. According to [19], all wire resistors R from every connected waveguide c_r of length $k_{c_r} + 1$ produce a noise power spectral density

$$P_{N,i,c_r,R}(f) = \frac{4KTRZ_L}{2|j2\pi f M_{c_r}|^2} \times \sum_{n=0}^{k_{c_r}} \left| \sum_{m=n}^{k_{c_r}} \frac{|S(x_{c_r}, x_{L,c_r}, n)|}{S(x_{c_r}, x_{L,c_r}, m) S(x_{c_r}, x_{L,c_r}, m+1)} \right|^2. \quad (22)$$

³Note that $Q_i \approx x_i^{k_i+1}$.

Additional noise results from the load impedance in transmitter circuits, corresponding to a power spectral density

$$P_{N,i,c_r,Tx}(f) = \frac{4KTZ_L^2}{2|j2\pi fM_{c_r}S(x_{c_r}, x_{L,c_r}, k_{c_r} + 1)|^2}. \quad (23)$$

Assuming again that the induced current in the first relay connected to the receiver is influenced by the magnetic field from the receiver coil in a much stronger manner than by the relays far away from the receiver due to the propagation distance, we calculate the power spectral density resulting from the noise in the load impedance in the receiver circuit using (17), which results in

$$P_{N,i,Rx}(f) \approx \frac{1}{2} \frac{4KTZ_L^2}{|j2\pi fM_i|^2} \times \frac{1}{\left| x_i + x_{L,i} - \frac{S(x_i, x_{L,i}, k_i - 1)}{S(x_i, x_{L,i}, k_i)} N_r \right|^2}, \quad (24)$$

where N_r is the number of the waveguide connections of the receiver node and index i indicates the considered waveguide. The resulting total noise power spectral density at the considered receiver is then given by

$$P_{N,i}(f) = P_{N,i,Rx}(f) + \sum_{c_r=1}^{N_r} P_{N,i,c_r,R}(f) + \sum_{c_r=1}^{N_r} P_{N,i,c_r,Tx}(f). \quad (25)$$

As it was studied in [19], direct MI transmission provides a large channel capacity only at a very low carrier frequency and a high number of windings of the coils. It can be shown that for the optimal parameters of the MI waveguide, the channel capacity of the direct MI transmission for coil distances above 15 m becomes very low, because the signal power at the receiver due to the direct link between the coils is equal to or below the power of the thermal noise. Therefore, the MI waveguides are highly directional and the number of interferers cannot be given by the number of the nodes inside the coverage area like it is done for the EM-waves based sensor networks [14], [18]. Moreover, the interfering signals may be propagated through the whole network and the number of interfering nodes depends on the topology, i.e., the connection of waveguides. However, for a given set of system parameters, only a small part of all interferer nodes needs to be taken into account, because the resulting path loss for the interfering signals may be very high, especially for the interferers, which are a large number of relays away from the receiver.

Due to the high path loss of the interference route for the j th interferer, we approximate it by an MI waveguide with maximum polarization factor $J = 2$ of length $k_{I,j} + 1$ coils (worst case approximation), where $k_{I,j} - 1$ is the number of passive coils on the interference route between the interfering node and the receiver. The interference power spectral density can be specified by

$$P_{I,i,j}(f) = \frac{P_{t,I,i,j}(f)}{L_{p,I,j}(f)}, \quad (26)$$

where $P_{t,I,i,j}(f)$ is the power spectral density of the interference source and $L_{p,I,j}(f)$ is the path loss of the interference route, which is similar to (21) and can be given by

$$L_{p,I,j}(f) \approx \frac{|S(\tilde{x}, \tilde{x}_L, k_{I,j}) \cdot \tilde{Q}|}{|\text{Im}\{\tilde{x}_L\}|} \cdot |2^{m-1}|^2, \\ \tilde{Q} = (\tilde{x} + \tilde{x}_L) \cdot S(\tilde{x}, \tilde{x}_L, k_{I,j}) - N_c \cdot S(\tilde{x}, \tilde{x}_L, k_{I,j} - 1), \quad (27)$$

where $\tilde{x} = \frac{Z}{j2\pi f\tilde{M}}$ and $\tilde{x}_L = \frac{Z_L}{j2\pi f\tilde{M}}$. Here, \tilde{M} stands for the mutual inductance between coils in 3 m distance (worst case assumption). An additional weight of 2^{m-1} is due to the load impedance $Z_L = R$ in every node of the interference route, yielding $\frac{Z+Z_L}{j2\pi f\tilde{M}} \approx \frac{2R}{j2\pi f\tilde{M}} = 2 \cdot \tilde{x}$ if $|Z - Z_L| \approx 0$, which is a realistic assumption due to transmission in a narrow band around f_0 , where $Z \approx R$ and $Z_L = R$. The interference power density is chosen in the same way like in (16) (worst case assumption).

B. Interference Management

One of the major goals of this work is to provide a comparison between the two schemes, direct MI transmission and MI waveguides based networks, at their optimal conditions with regard to the bottleneck throughput. In order to determine which solution is better, we need a precise definition for the throughput metric, especially concerning the number of interfering nodes, which may dramatically affect the number of scheduled data streams, the available data rate at the bottleneck link and therefore the total throughput. Similarly to [1] and [2], we assume that some of the interfering signals can be avoided by establishing a multinode scheduling. The remaining interfering signals provide additional disturbance for the transmitted signal. Hence, unlike in previous works, we determine the number of interfering nodes $N_{\text{interferers},i}$, which need to be taken into account in scheduling, such that the available data rate of a corresponding link i is maximized.

The problem of maximizing the available data rate of link i can be formulated as follows:

$$\max_{\forall D_1, D_2} \frac{\int_{-\infty}^{+\infty} \log_2 \left(1 + \frac{P_{t,i}(f)}{L_{p,i}(f) \cdot P_{\text{disturb},i}(f)} \right) df}{1 + \sum_{j \in D_2} 1}, \\ \text{s.t. : (1) } D_1 \cup D_2 = D, \quad (2) \quad D_1 \cap D_2 = \emptyset, \quad (28)$$

where $P_{\text{disturb},i}(f) = E\{P_{N,i}(f)\} + \sum_{j \in D_1} P_{I,i,j}(f)$. D contains the indices from all nodes, which can interfere with transmissions of link i . D_2 is a subset of D and contains only interferers, which are considered in the aforementioned multinode scheduling,⁴ i.e., which finally will not create a disturbance to the considered link. D_1 contains the indices of the remaining interferers. Here, the channel capacity from (11) is divided by

⁴The interfering signals are separated by means of TDMA. Then, the own data is transmitted only in each $(1 + N_{\text{interferers},i})$ slot and the maximally available data rate decreases by this factor.

$(1 + N_{\text{interferers},i}) = 1 + \sum_{j \in D_2} 1$ due to the scheduling. According to (28), the available data rate is maximized by finding an optimal separation of D in D_1 and D_2 . It can be easily shown, exploiting the fact that all interferer power densities have approximately the same shape, that $\max_{j \in D_1} \int_{-\infty}^{+\infty} P_{I,j}(f)df \leq \min_{j \in D_2} \int_{-\infty}^{+\infty} P_{I,j}(f)df$ holds. Therefore, D_1 and D_2 can be found iteratively by storing all interferers in D_1 and moving the strongest interferer one by one to D_2 . In each iteration the resulting available data rate is calculated using (28) and the partitioning with the maximal data rate is chosen. Using the optimal D_1 and D_2 , the number of relevant interferers $N_{\text{interferers},i}$ and the modified channel capacity $C_{ch,i}$ can be determined.

III. THROUGHPUT MAXIMIZATION

If every link operates on a different frequency, an individual design of all circuits (nodes and possibly relays) for this link is needed. Each node needs then as many circuits and therefore coils, as links are connected to it. Such a system becomes impractical with increasing number of nodes, especially in case of MI waveguides based networks. Therefore, we propose to choose a set of system parameters, which are identical for all used circuits. The optimal solution maximizing the throughput of the network may depend on the topology of the network, which is discussed in the following as well. In this work we focus on spanning trees as a special case of the network topology [32]. A fully connected spanning tree is a graph, which connects multiple nodes such that one and only one route between any two nodes exists. This approach is beneficial compared to circular connected trees (with possibly more than one route between any two nodes). The circularity of the network needs to be avoided, because the old data may disturb the transmission of the current data in an unpredictable way.

As discussed earlier, the traffic load has to be less or equal to the available data rate at the node. In case of equality between the maximum available data rate and the traffic load, the throughput T_i of a link is as follows according to [18] and [2]:

$$T_i = \frac{C_{ch,i}}{N_{\text{routes},i} \cdot (1 + N_{\text{interferers},i})}, \quad (29)$$

where $C_{ch,i}$ is the channel capacity of link i , $N_{\text{routes},i}$ is the number of data streams of link i and $N_{\text{interferers},i}$ is the number of interfering nodes included into the scheduling. The number of relevant interferer nodes for a particular link depends on the interference powers received from the different nodes, hence, on the system parameters and the network topology. Note, that $C_{ch,i}$ and $N_{\text{interferers},i}$ of a practical system may vary with the time-varying channel conditions, such that the system may need to adapt to it. However, the adaptivity of a practical system is beyond the scope of our work. In addition, if the statistics of the medium properties are available, e.g., in terms of a statistical distribution of the soil conductivity, the throughput metric T_i in (29) can be replaced by the expectation value with respect to

the medium dependent throughput distribution. For simplicity, constant medium properties are assumed in this work.

In the following, we present the most promising optimization techniques, which maximize the bottleneck throughput of the network. At first, we formalize the optimization problem and then we show the key techniques, which provide a suboptimal but close-to-optimum solution.

A. Problem Formulation

The optimization problem can be formulated as follows:

$$\begin{aligned} & \max_{\forall f_0, N, V, M_{\text{links}}} \min_i T_i, \\ \text{s.t. : } & (1) P_i = P \forall i, (2) \frac{1}{(2\pi f_0)^2 L} \geq C_0, \end{aligned} \quad (30)$$

where f_0 is the carrier frequency (identical for all links) and N is the number of windings (equal for all used coils). M_{links} corresponds to a set of links, which form a fully connected spanning tree and i stands for a particular link of this tree. T_i is the throughput according to (29). In addition, we assume equal transmit power in all nodes (constraint (1), P_i : transmit power of i th node) and that the smallest used capacitance is bounded by C_0 , cf. [19] (constraint (2)). The matrix $V \in \mathbb{R}^{3 \times N_{\text{coils}}}$ contains the direction vectors of all coils expressed in Cartesian coordinates, where N_{coils} denotes the total number of MI enabled devices including transceivers and relays.

As it is shown in [19], finding the optimal system parameters for maximizing the channel capacity of an MI-link is a non-convex problem, which cannot be solved using convex optimization tools from [33]. Because the problem in [19] is obviously a subproblem of (30), (30) is also non-convex.

B. Optimal System Parameters

The optimization of the available system parameters is very important, because as it was shown in previous works, in several cases no transmission can be established when operating, e.g., in the wrong frequency range. As it was shown in [19], system parameters like f_0 and N need to be optimized to achieve the maximum channel capacity. In [19] this optimization is performed using a multiscale search in the two-dimensional parameter space. However, this algorithm is inaccurate, because f_0 is a continuous variable. Due to the different properties of the MI waveguides compared to the direct MI based transmissions, the optimal set of system parameters differs substantially for both schemes and we have to determine them independently.

1) *Direct MI Transmission:* For direct MI transmissions, the optimal number of windings N reaches its maximum value N_{max} , because of the low optimal carrier frequency, which is below the bound given by the capacitor constraint as results from [19]. Therefore, we eliminate this variable from the optimization. Due to a large distance between the transceivers and therefore a very low mutual inductance of the direct MI transmission based links, (12) can be approximated by

$$L_{p,i}(f) \approx \left| \frac{R}{j2\pi f M_i} \right|^2. \quad (31)$$

As discussed in [19], the loss factor G in (3) can be determined according to $G = \exp(-\frac{r}{\delta})$, where δ denotes the skin depth. In addition, the approximation of the skin depth $\delta \approx \frac{1}{\sqrt{f_0 \pi \sigma \mu}}$ is valid. The path loss in (31) close to the carrier frequency can be minimized, if $|j2\pi f_0 M_i|$ is maximized. Since J from (6) does not depend on f , we take it out of the optimization of the system parameters. Thus, using (3) and (4) we obtain

$$f_0 M_i \propto f_0 \cdot \mu \pi N^2 \frac{a^4}{4r_i^3} \exp(-r_i \sqrt{f_0 \pi \sigma \mu}). \quad (32)$$

The maximum of this function with respect to f_0 is given by

$$f_0 = \left(\frac{2}{r_i \sqrt{\pi \sigma \mu}} \right)^2. \quad (33)$$

However, due to the different lengths of the links, the optimal carrier frequency results from a tradeoff between the different optimal frequencies of all available links. The search for the optimal frequency should be therefore performed in the range $[f_{\min}, f_{\max}] = \left[\left(\frac{2}{r_{\max} \sqrt{\pi \sigma \mu}} \right)^2, \left(\frac{2}{r_{\min} \sqrt{\pi \sigma \mu}} \right)^2 \right]$, where r_{\min} and r_{\max} denote the minimum and maximum transmission distance in the network, respectively. In this range, a grid is spanned and further parameters (orientations of coils and network topology) are optimized to maximize the throughput for each point of the grid. The point with the largest throughput indicates the best carrier frequency.

2) *MI Waveguides*: For MI waveguides, we exploit the property of the waveguides, that the optimization under the capacitor constraint according to [19] leads to a significant degradation of the channel capacity. However, the capacitor constraint results from a realistic restriction of the capacitor capacitance in a practical system and needs to be taken into account. It was shown that with increasing carrier frequency and/or increasing number of windings the channel capacity increases monotonically. Therefore, the optimal solution meets the capacitor constraint with equality. Hence, we can express the optimum f_0 as a function of N :

$$C_0 = \frac{1}{(2\pi f_0)^2 L(N)} \Rightarrow f_0 = \frac{1}{2\pi \sqrt{L(N)C_0}}, \quad (34)$$

where $L(N)$ indicates that the inductivity L depends on N . With this information, the optimization problem for MI waveguides in [19] could be solved using a full search in one integer variable N . Correspondingly, the complexity of (30) reduces since one variable can be eliminated.

C. Network Polarization

1) *Direct MI Transmission*: The throughput of the direct MI transmission based network can be greatly improved, if the number of interfering nodes is reduced. We exploit the polarization property of the coils, in order to reduce the number of relevant interferers. The motivation for this technique is due to the fact, that the polarization factor J from (6) becomes zero for several combinations of the angles θ_t , θ_r , and ϕ , e.g., if

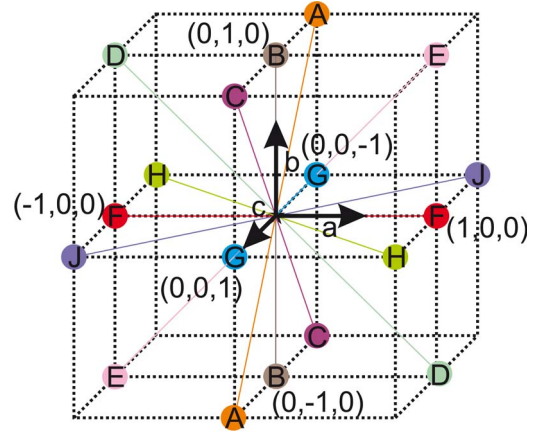


Fig. 4. Possible coil axes' directions.

$\theta_t = 0$ and $\theta_r = \pi/2$. In a practical system, the deployment of coils cannot be done with an infinite precision. Hence, the separation of the possible directions for the coil axis should not be too small, since otherwise the angle deviation due to the deployment may be larger than this angle separation, which is of course not reasonable. Therefore, we assume an angle separation of at least 45° between any two possible directions. This ensures that small deviations from the optimal directions become negligible and do not change the system behavior. A map of possible directions can be then visualized using a cube, like in Fig. 4. The coordinates of each point are specified in the vector space given by the basis vectors \vec{a} , \vec{b} , and \vec{c} , and correspond to a possible direction of the coil. Obviously, there are 9 pairs of points.⁵ For each pair, the two points correspond to the opposite directions on the same axis. Therefore, the absolute value of the polarization factor and the path loss according to (31) remain the same, and the total number of different vectors is reduced to 9.

The optimal solution for the orientation of the coils can be found by applying a full search over all $9^{N_{\text{nodes}}}$ possible combinations. Due to the non-convexity of the original problem and the discrete orientation of the coils, it is not possible to determine the solution without taking into consideration all possible constellations. Thus, the computational effort increases exponentially with the number of nodes in a network, such that the optimization becomes impractical for a network with $N_{\text{nodes}} > 10$. Therefore, we propose an iterative algorithm for improving the minimum throughput. For this, we start with the calculation of the throughput metric for all links with the coils rotated to the surface (default state). The link with the least throughput is selected as the worst link and the minimum throughput is stored for performance comparison. In the algorithm initialization phase, we define the basis vectors \vec{a} , \vec{b} , and \vec{c} . Selecting one of the vectors, e.g., \vec{a} , identical with the transmission direction of the worst link, we make sure that the path loss of this worst link can be reduced at least by the horizontal axes deployment gain compared to the default state [19] (the polarization factor in (6) and therefore the mutual inductance in (3) double compared to the vertical

⁵In Fig. 4, every two points, which belong to the same pair, are marked with the same color and letter.

axes deployment). We choose the second vector (e.g., \vec{b}) to point to the ground surface, yielding the default state to be available as a possible solution, too. The third vector \vec{c} is then orthogonal to the given vectors \vec{a} and \vec{b} . In each iteration, the closest $N_x - 1$ ($N_x = 5$ for our numerical results) nodes to the receiver node of the worst link and the receiver node itself are selected and for these nodes all 9^{N_x} constellations are investigated. The optimal combination is found, which maximizes the least throughput metric among all links of the network. The corresponding link is selected for the next iteration. This strategy ensures a monotonic increase of the throughput from step to step. The algorithm stops, if the worst link remains the same as the original worst link of this iteration, which means, that no further gain can be achieved.

2) *MI Waveguides*: For the MI waveguides based networks, the orientation of the sensor coils may not vary. Otherwise, a difference in polarization of transmitter and receiver nodes may dramatically affect the signal propagation properties within the waveguide, yielding strong power reflections and reducing the channel capacity. Therefore, we assume that each pair of coils in a waveguide is rotated in the same direction. Hence, in a spanning tree based network, all coils' axes point in the same direction, and for the polarization factor J from (6) $J \geq 1$ is valid. Due to a strong coupling between coils in waveguides, interfering signals cannot be avoided by this strategy. However, the power of the useful signal and therefore the channel capacity can be improved by the proper choice of the coil orientation. Specifically, the drawback of the vertical deployment scheme (default state) was pointed out in [19] and [2]. Using an approximated path loss function, it can be shown that the path loss of the vertically deployed MI waveguide is significantly larger than that of the horizontally deployed (all coils rotated towards each other) MI waveguide. This effect becomes dramatical with increasing transmission distance and number of relays. Therefore, it is essential to optimize the coils' orientations in order to reduce the path loss and increase the channel capacity of the bottleneck link.

Since all sensor nodes can only be rotated at once as already discussed, there are only 9 possible combinations according to the structure in Fig. 4, which can be investigated one by one. Since the vertical deployment neither improves the channel capacity nor reduces the interference power, not all 9 combinations from Fig. 4 need to be investigated, but only 4 which lie in the plane parallel to the surface.

D. Network Topology

The minimum spanning tree (MST) corresponds to a weighted graph (each weight represents, e.g., the transmission distance between two sensor nodes), which connects all nodes of a network and has the minimum sum of weights among all possible graphs. It can be found using the iterative method of Prim [34]. Unfortunately, we cannot use (29) as weight for the graph of nodes to be connected, because this preassumes the knowledge about the network topology for the calculation of the numbers of routes and interferers. Hence, it is not possible to optimize the throughput directly. It has been shown in [35], that the MST solution minimizes not only the sum of the weights,

but also the maximum weight occurring in the tree. Hence, the MST can be approximately viewed as a spanning tree with nodes connected to their closest neighbors, if the weights are chosen according to the transmission distance. However, since the MST approach does not involve the traffic load for the calculation of the spanning tree, the resulting network topology may not be optimal in terms of the metric given in (29).

1) *Direct MI Transmissions*: For direct MI transmission based networks, it is intuitive that the distance between the nodes can be used as weights of the network graph for the calculation of the MST. With this approach, the maximum transmission distance and therefore the maximum path loss among all involved links is minimized. Alternatively, the number of relevant interferers can be calculated for any possible edge of the tree and used as weights for determining the MST. This approach minimizes the maximum number of interferers and is therefore called the minimum interference tree (MIT) [36]. However, according to our observations, this strategy does not yield any significant gain, because by minimizing the maximum number of interferers per link, links with larger path loss are still tolerated. Therefore, we focus on the distance-based MST as a network topology, which remains unchanged throughout the optimization. Hence, M_{links} is chosen according to this default scheme.

The problem in (30) is split into two subproblems:

$$1) T_{opt} = \max_{f_0} Y(f_0), \quad (35)$$

$$2) Y(f_0) = \max_V \min_i \{T_i\}, \quad (36)$$

where $Y(f_0)$ can be determined for a given value of the resonance frequency f_0 by applying the proposed polarization algorithm. T_{opt} is determined by establishing a grid of points in f_0 and searching for the maximum among the throughput values, which correspond to the points of the grid.

2) *MI Waveguides*: For MI waveguides based networks, we propose to use the number of relays in MI waveguides as weights, which minimizes the total number of used relay devices, cf. [18]. However, this approach may not maximize the throughput. Also, the metric given in (29) cannot be applied, because the number of interferers in MI waveguides based networks depends on the topology, which is yet unknown.

It has been observed in [19] that due to a suboptimal frequency of MI waveguides and the aforementioned capacitor constraint, even an MI waveguide with a high relay density behaves like a weakly coupled waveguide with a small bandwidth and its path loss function can be approximated by $|x|^{2k}$. Further approximations exploit the narrowband transmission and a relatively low level of the thermal noise, resulting in

$$C_{\text{ch},i} \approx B \cdot \log_2 \left(\frac{U_i}{|x_i|^{2k_i}} \right),$$

$$U_i = \frac{1}{B} \int_{f_0-0.5B}^{f_0+0.5B} \frac{P_{t,i}(f)}{P_{N,i}(f)} df, \quad (37)$$

where B is the bandwidth⁶ and $x_i \approx x \forall i$ yielding $U_i \approx U \forall i$. This equation can be transformed into

$$C_{\text{ch},i} \approx B \log_2(U) - 2B \cdot \log_2(|x|) \cdot k_i. \quad (38)$$

Hence, the sum of channel capacities can be expressed as

$$\sum_i C_{\text{ch},i} \approx (N_{\text{nodes}} - 1)B \log_2(U) - 2B \cdot \log_2(|x|) \cdot \sum_i k_i. \quad (39)$$

Therefore, by minimizing the total number of relays, which is given by $\sum_i k_i$, the sum of channel capacities over all links is maximized. Since the MST minimizes the maximum weight occurring in the tree [35], the minimum link capacity is maximized with the same approach. We assume a uniform distribution of the nodes, such that a uniform distribution of the routes and interferers can be assumed, yielding similar values among all links for N_{routes} and $N_{\text{interferers}}$. Under these assumptions, the maximization of the bottleneck throughput corresponds to the maximization of the minimum channel capacity. The problem (30) then can be split into three subproblems:

$$1) T_{\text{opt}} = \max_N Y_1(N) \quad (40)$$

$$2) Y_1(N) = \max_V Y(N, V), \quad (41)$$

$$3) Y(N, V) = W_1(N, V) - W_2(N, V) \cdot \min_{M_{\text{links}}} \max_i k_i, \quad (42)$$

where $W_1(N, V) = \frac{B \cdot \log_2(U)}{N_{\text{routes}} \cdot (1 + N_{\text{interferers}})}$ and $W_2(N, V) = \frac{2B \cdot \log_2(|x|)}{N_{\text{routes}} \cdot (1 + N_{\text{interferers}})}$. Here, the width of the low path loss band B and the factor $\log_2(|x|)$ depend on the coil polarization, which is indicated by an additional variable V in the brackets compared to the problem formulation in [2]. If the network tree is a weighted graph and its weights are set to k_i , which is equivalent to the transmission distance, then the solution for (42) is given by the MST. This MST is approximately identical to the MST with distance metric used for direct MI transmission based approach since the number of relays $k_i - 1$ essentially is proportional to the distance. Hence, this approach is an optimal solution for the given assumptions. As explained earlier, the subproblems (40) and (41) are solved via a full search in variable N and among all possible coil directions, respectively.

The above discussion on the MST is based on the approximations of the channel capacity and that of the number of interferers and routes in a network. However, due to a random distribution of nodes and further optimization of the system parameters, there might be cases, where the numbers of interferers and routes are not equal for all nodes and also cases, where the system is operated at frequencies, at which the above approximations are only partially valid. Then, the MST becomes a suboptimal approach, which performs, however, still

close to the optimum. The optimal solution for the topology can be given by performing a full search over all possible spanning trees for the given node positions. However, the corresponding effort becomes very high with increasing number of nodes. Therefore, we propose an iterative algorithm, which finds a better solution than the default scheme with significantly reduced complexity.

The starting point for the algorithm is an MST. For the initial calculation of the MST, every node is allowed to be connected to every other node. We calculate the throughput for all links of the system, list them in increasing order, and store their indices in lists L_c and $L_{c,\text{min}}$. In addition, an empty list $L_{\text{forbidden}}$ is created in order to save the links, which will be excluded from the computation. For the following steps, $L_{c,\text{min}}$ remains unchanged, because it is used as a reference for the extended search, see below.

In each iteration, the first link from L_c is taken. In the given constellation this link is not only disturbed by a high amount of interference and loaded by a high number of information streams, due to symmetry, it also provides interference to a high number of nodes and loads its direct receiver node with a high number of streams to be served. Therefore, this link is said to be the most disturbing one. Hence, we exclude it from the MST finding procedure by setting the number of relays between the corresponding nodes to infinity and saving the link's index in $L_{\text{forbidden}}$. This link is then avoided by the Prim's algorithm. Then, we calculate a new MST and L_c . If the minimum throughput of the new tree is higher than the highest minimum throughput obtained so far, the new tree is stored as a candidate for the optimal solution.

We observe that if the number of links, which are connected to the same node and stored in $L_{\text{forbidden}}$, is higher than X_f (e.g., $X_f = 5$ in our numerical results), this central node is likely to be connected to a node beyond its closest neighborhood. Hence, the path loss of the corresponding link dramatically increases and no further improvement can be achieved. Therefore, we consider this as a stopping criterion. This strategy usually leads to an increase of the network throughput. However, the resulting tree depends on the choice of the first forbidden link, which determines all further steps of the algorithm. Since it may happen that the worst link by means of the network throughput is not the most disturbing one (due to, e.g., low channel capacity and low number of relevant interferers and routes), we also need to investigate the cases, where the algorithm starts with any other link as a forbidden connection. After each stop due to too many forbidden connections of one link (as described above), $L_{\text{forbidden}}$ is cleared and the second element from $L_{c,\text{min}}$ is taken as the first forbidden link. The optimization terminates after X_I iterations or if all elements from $L_{c,\text{min}}$ have been used once as the first forbidden link. The stored tree with the highest network capacity is returned. We call this method an advanced spanning tree (AST) approach.

IV. NUMERICAL RESULTS

In this section we present numerical results in terms of throughput and throughput gain for randomly generated networks.

⁶The optimal bandwidth results from the water filling approach and differs from network to network.

In our simulations, we assume a total transmit power of $P = 10$ mW per node. Furthermore, we utilize coils with wire radius 0.5 mm and coil radius 0.15 m. The conductivity and permittivity of dry soil are, respectively, $\sigma = 0.01$ S/m and $\epsilon = 7\epsilon_0$, where $\epsilon_0 \approx 8.854 \cdot 10^{-12}$ F/m. Since the permeability of soil is close to that of air, we use $\mu = \mu_0$ with the magnetic constant $\mu_0 = 4\pi \cdot 10^{-7}$ H/m. In most applications of WUSNs, the density of sensor nodes needs to be high to ensure that enough sensed information is collected. However, as it was shown in [3], [19], with a small distance between two nodes, MI based transmission is outperformed by EM waves based transmission. Therefore, we consider randomly deployed nodes with the minimum distance between any two nodes not less than 21 m in order to provide a scenario, where MI based transmission yields a better performance than the traditional EM waves based transmission. We assume a square field of size $F_x \times F_x$, yielding a total area F_x^2 . Within this field, a random uniformly distributed set of N_{nodes} sensor nodes is generated for each network optimization. In this set, a root node is selected, which is the closest node to the lower left field corner. This node may have a connection to the aboveground devices, which then retransmit the collected information. In order to examine the benefits of the proposed optimization techniques, we show the minimum throughput distributions and throughput gains for 100 randomly deployed sensor networks using either MI waveguides based transmissions or direct MI based transmissions. Furthermore, these 100 networks are obtained assuming three different scenarios, respectively:

- $N_{\text{nodes}} = 20$, $F_x^2 = 0.01$ km²,
- $N_{\text{nodes}} = 20$, $F_x^2 = 0.04$ km²,
- $N_{\text{nodes}} = 40$, $F_x^2 = 0.04$ km².

This allows for conclusions with respect to the impact of an increase of the number of sensors while keeping a constant field size and an increase of the field size while keeping a constant number of sensors, respectively.

As a default scheme for comparison, we utilize the so-called vertical axes deployment according to [18], where the coil axes are rotated to the ground surface.

For this case, an optimization of the system parameters is also needed according to our derivations in Section III-B. This part of the optimization is applied to the default scheme in order to ensure a fair comparison between the proposed solution and the default scheme. In addition, we establish the network topology for the default scheme by means of the minimum spanning tree, which already provides near optimum performance in terms of metric (29) as pointed out in [2]. However, as explained in Section III, the default scheme serves as a starting point for the proposed further optimization, hence, a throughput gain is expected at the cost of additional computational effort.

A. Direct MI Transmissions

For direct MI transmission, our optimization results in resonance frequencies ranging between 10 kHz and 250 kHz and bandwidths between 1 kHz and 25 kHz.

In Fig. 5, we observe a large gap in throughput between the deployment in 0.01 km² and in 0.04 km² field. This is

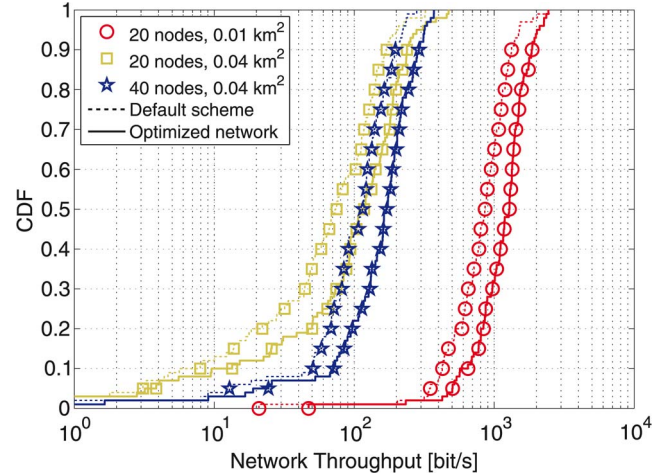


Fig. 5. Throughput of direct MI transmission based random WUSNs.

due to the increased average transmission distance, such that the path loss of the bottleneck link in the latter scenario is dramatically higher. The minimum available data rate for the optimized solutions with 20 nodes and 0.01 km² is ≈ 47 bit/s. However, much higher data rates can be achieved for this scenario, depending on the deployment of nodes up to 2.45 kbit/s. On the other hand, for deployment in 0.04 km² field, the bottleneck throughput can be very low. In particular, we show only results for the throughput above 1 bit/s. However, due to the optimization, these low data rates occur only in 2–3% of cases. Furthermore, we observe that the throughput for the proposed solution increases with increasing number of sensor nodes and a constant field size. This results from the applied interference polarization technique, which makes the performance mainly dependent on the channel capacity, which is significantly larger with shorter transmission ranges.

Although our optimization goal is maximizing the bottleneck throughput, it is also interesting to investigate, how much information can be collected by the sink node per second. For this, we need to multiply the throughput with the number of packets, which can be successfully received by the sink. Due to assumed no loss of data packets, we can deduce that all packets transmitted to the sink from all sensor nodes connected to it can be successfully received, such that the resulting number of packets corresponds to the number of routes of the sink, given by⁷ $N_{\text{routes},1} = N_{\text{nodes}}$. Therefore, in the considered scenarios, we multiply the bottleneck throughput with either 20 or 40, in order to obtain the available data rate of the sink. These data rates are bounded below by 49 kbit/s for the deployment in 0.01 km² field, by 9.4 kbit/s for 20 nodes deployed in 0.04 km² and by 14.8 kbit/s for 40 nodes in 0.04 km².

B. MI Waveguides Based Transmissions

For the MI waveguides based WUSNs, the optimum resonance frequencies lie in the range between 1 MHz and 10 MHz, and bandwidths between 150 Hz and 500 Hz are optimum. A large gain can be obtained due to the network polarization

⁷The number of routes of the sink node includes its own sensed data. If sink node is not occupied with a sensor, then the number of routes decreases by one.

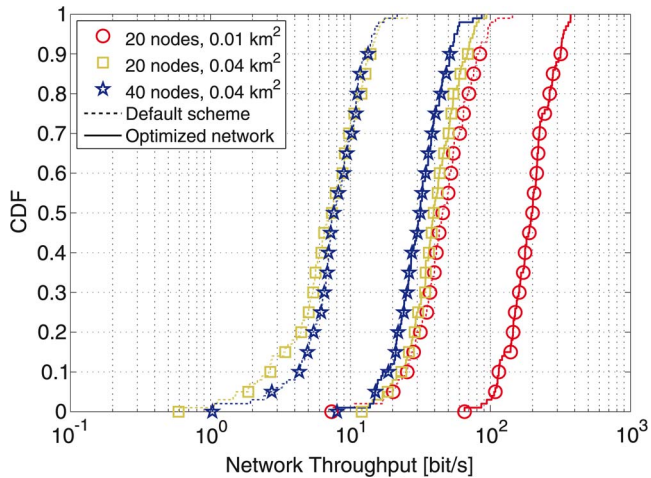


Fig. 6. Throughput of MI waveguides based random WUSNs.

strategy, which improves the coupling between each two adjacent coils of the waveguide, cf. [19]. Therefore, the resulting channel capacity can be dramatically increased, if a proper orientation of the coils is chosen. However, this approach does not reduce the number of relevant interfering nodes to be scheduled and the number of data streams to be served by the worst link, which is done using the AST approach.

In Fig. 6, we present a cumulative distribution of the minimum network throughput. We observe a large gap between the proposed solution and the default scheme similarly to the direct MI transmission based networks. This is due to the cases, where the random positions of the sensors are very unfortunate for the communication, e.g., if a set of sensors is deployed very close to the upper right field corner and the remaining sensors are deployed close to the lower left field corner. In such cases, the two groups of sensors are connected via a very long MI waveguide, such that the resulting path loss is very large. In addition, the corresponding receiver of the worst link may belong to a group of nodes, which are placed very close to each other. Hence, the surrounding nodes have a lower path loss than the worst link and inject high power interference signals. This has to be circumvented by scheduling. Therefore, the resulting number of interfering nodes for such links is also very large, thus dramatically decreasing the minimum throughput. In contrast, the proposed solution can greatly improve the performance by reducing the path loss and by choosing a better topology. Furthermore, the path loss of the proposed solution reduces compared to the default scheme exponentially with the transmission distance, cf. [19], such that huge throughput gains are expected for such constellations.

The proposed solution does not lead to high data rates for the given scenarios, however, we observe the minimum throughput for the worst case to be bounded above 65 bit/s with 20 nodes and 0.01 km². Interestingly, with an increased number of nodes and a constant field size the resulting throughput for the proposed solution decreases, although shorter transmission distances between the nodes are supposed to lower the path loss and improve the performance. Instead, due to the increased number of interfering signals and data streams, the resulting throughput for a larger number of nodes becomes lower.

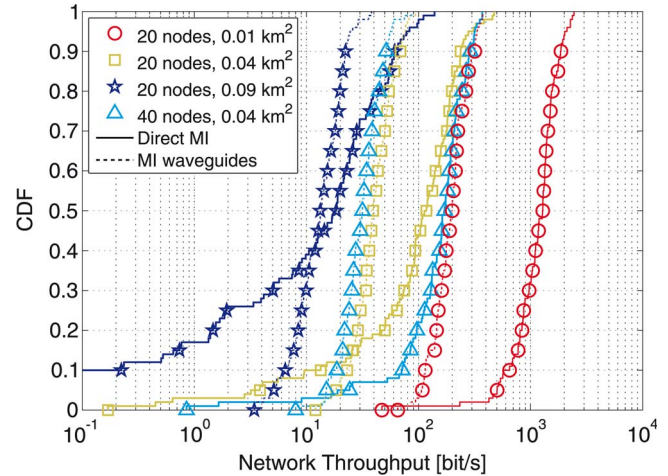


Fig. 7. Comparison of the proposed solutions in terms of resulting throughput.

However, the performance difference is not large, which is due to the applied AST approach, which helps to determine a topology with a reduced impact of interference and traffic load. With increasing field size (from 0.01 km² to 0.04 km²) and a constant number of nodes, the minimum throughput decreases dramatically. We observe very large gains, especially for the deployment in a 0.04 km² field. For 47% of the cases with 20 nodes and for 22% of the cases with 40 nodes, the throughput gain reaches values beyond 500%. The reason is, as mentioned earlier, that for an unfortunate distribution of nodes the worst link of the default scheme suffers from a large path loss and a high number of interfering signals. Hence, even for the resulting low data rates of the proposed solution the throughput gain becomes very large. For the deployment in a 0.01 km² field, the throughput gains are lower. However, for 50% of the networks, a throughput gain above 310% can be achieved. For more than 10% of the cases, a gain of more than 680% is observed. On average, a gain of 370% can be expected, which leads to a throughput higher by more than a factor of four.

Similarly to Section IV-B, we calculate the available data rate at the sink node by multiplying the resulting bottleneck throughput with the number of data packets, which can be received by the sink. For the deployment in the 0.01 km² field, we obtain an available data rate of up to 7.5 kbit/s. With 20 and 40 nodes deployed in the 0.04 km² field, data rates of up to 1.9 kbit/s and 3.46 kbit/s, respectively, result.

C. Comparison

One of the remaining questions is, which scheme performs better, MI waveguides or direct MI transmissions. We try to answer this question using Fig. 7. For a more comprehensive comparison, we show not only the results for the network constellations described above, but also for the deployment of 20 sensor nodes in a large field of 0.09 km² area. For the deployment in 0.01 km² field, we observe that the direct MI transmission based WUSNs mostly outperform the MI waveguides based WUSNs. Therefore, the deployment of additional passive relays between the transceiver nodes is not recommended for such networks. For the deployment of 20 nodes in 0.04 km²,

the direct MI transmission is more beneficial in $\approx 75\%$ of cases according to our simulations. The achievable throughput gain reaches a value of 400%. However, for the remaining 25% of cases, the MI waveguides outperform the direct MI transmission based schemes. For the networks with 40 nodes, direct MI transmission based WUSNs perform better than the MI waveguides based WUSNs in 97% of cases. Finally, for the deployment in 0.09 km² field, we observe that MI waveguides outperform the direct MI transmission in 40% of cases. In many cases, no reasonable throughput values (e.g., $\approx 10^{-3}$ bit/s) can be obtained using direct MI transmission. Thus, under the given assumption, MI waveguides can be considered the only feasible solution, although the achievable bottleneck throughput is very low, at most 12 bit/s, which corresponds to an available data rate at the sink node of 240 bit/s. Furthermore, we observe, that the throughput of the direct MI transmission based WUSNs reduces much faster with increasing deployment field and therefore with the average transmission distance between any two sensor nodes (please compare the respective results for MI waveguides and direct MI transmission with 20 nodes and different fields sizes).

Although there are cases, when MI waveguides provide significantly better performance, it is necessary to keep in mind that a much higher deployment effort is needed for such schemes. As an example, the average number of devices to be deployed in 0.01 km² field with only 20 sensor nodes is more than 130, which comes in addition to the 20 sensor devices being the only devices to be deployed in direct MI transmission based WUSNs. This is a considerable drawback of the MI waveguides, thus making the system expensive and less flexible. In 0.04 km² field with 20 nodes, the number of passive relay devices is more than 300 and for the deployment in 0.09 km² it is more than 450. Hence, in most of the constellations, the deployment effort and costs of the WUSNs with waveguides are very high.

V. CONCLUSION

In this paper, we have presented optimization techniques for the two most important cases of magnetic induction based WUSNs, MI waveguides and direct MI transmission based WUSNs. The main goal of this work was to provide bounds for the throughput of such networks. For this purpose, we have derived new channel, noise, and interference models, which differ from the existing models and incorporate all relevant signal reflections which occur in magnetic induction based communication systems. As an important step towards the practical realization of this kind of networks, we include some practical constraints into the formalization of the optimization problem, e.g., the unification of the system parameters and deployment precision restrictions. Finally, we have compared the resulting network throughput for direct MI transmission based WUSNs with that of MI waveguides based WUSNs. From our observations we can conclude, that in some cases, especially if the average transmission distance between nodes is not too large, the MI waveguides based WUSNs do not provide a better performance, as expected from the motivation given by the previous works in this field. In other cases, a large

throughput gain compared to the direct MI transmission based WUSNs is observed. However, this gain is reached at the price of a much higher deployment effort and less flexibility of the system.

REFERENCES

- [1] S. Kisseleff, I. F. Akyildiz, and W. Gerstacker, "Interference polarization in magnetic induction based wireless underground sensor networks," in *Proc. IEEE 24th Int. Symp. PIMRC*, Sep. 2013, pp. 71–75.
- [2] S. Kisseleff, W. Gerstacker, Z. Sun, and I. F. Akyildiz, "On the throughput of wireless underground sensor networks using magneto-inductive waveguides," in *Proc. IEEE GLOBECOM*, Dec. 2013, pp. 322–328.
- [3] I. F. Akyildiz, Z. Sun, and M. C. Vuran, "Signal propagation techniques for wireless underground communication networks," *Phys. Commun.*, vol. 2, no. 3, pp. 167–183, Sep. 2009.
- [4] I. F. Akyildiz, W. Su, Y. Sankarasubramaniam, and E. Cayirci, "Wireless sensor networks: A survey," *Comput. Netw.*, vol. 38, no. 4, pp. 393–422, Mar. 2002.
- [5] I. F. Akyildiz and E. P. Stuntebeck, "Wireless underground sensor networks: Research challenges," *Ad Hoc Netw.*, vol. 4, no. 6, pp. 669–686, Nov. 2006.
- [6] J. I. Agbinya and M. Masihpour, "Near field magnetic induction communication link budget: Agbinya–Masihpour model," in *Proc. 5th IB2Com*, 2010, pp. 1–6.
- [7] J. I. Agbinya and M. Masihpour, "Power equations and capacity performance of magnetic induction communication systems," *Wireless Pers. Commun.*, vol. 64, no. 4, pp. 831–845, Jun. 2012.
- [8] M. Masihpour, D. Franklin, and M. Abolhasan, "Multihop relay techniques for communication range extension in near-field magnetic induction communication systems," *J. Netw.*, vol. 8, no. 5, pp. 999–1011, May 2013.
- [9] K. Lee and D.-H. Cho, "Maximizing the capacity of magnetic induction communication for embedded sensor networks in strongly and loosely coupled regions," *IEEE Trans. Magn.*, vol. 49, no. 9, pp. 5055–5062, Sep. 2013.
- [10] Z. Sun and I. F. Akyildiz, "Magnetic induction communications for wireless underground sensor networks," *IEEE Trans. Antennas Propag.*, vol. 58, no. 7, pp. 2426–2435, Jul. 2010.
- [11] E. Shamonina, V. A. Kalinin, K. H. Ringhofer, and L. Solymar, "Magneto-inductive waveguide," *Electron. Lett.*, vol. 38, no. 8, pp. 371–373, 2002.
- [12] R. R. A. Syms, I. R. Young, and L. Solymar, "Low-loss magneto-inductive waveguides," *J. Phys. D, Appl. Phys.*, vol. 39, no. 18, pp. 3945–3951, Sep. 2006.
- [13] E. Shamonina, V. A. Kalinin, K. H. Ringhofer, and L. Solymar, "Magnetoinductive waves in one, two, and three dimensions," *J. Appl. Phys.*, vol. 92, no. 10, pp. 6252–6261, Nov. 2002.
- [14] P. Gupta and P. R. Kumar, "The capacity of wireless networks," *IEEE Trans. Inf. Theory*, vol. 46, no. 2, pp. 388–404, Mar. 2000.
- [15] C.-X. Wang, X. Hong, H. H. Chen, and J. Thompson, "On capacity of cognitive radio networks with average interference power constraints," *IEEE Trans. Wireless Commun.*, vol. 8, no. 4, pp. 1620–1625, Apr. 2009.
- [16] B. Liu, Z. Liu, and D. Towsley, "Capacity of a wireless ad hoc network with infrastructure," in *Proc. 8th ACM Int. Symp. Mobile Ad Hoc Netw. Comput.*, Sep. 2007, pp. 239–246.
- [17] A. Spyropoulos and C. S. Raghavendra, "Capacity bounds for ad-hoc networks using directional antennas," in *Proc. of IEEE ICC 2003*, May 2003.
- [18] Z. Sun and I. F. Akyildiz, "On capacity of magnetic induction-based wireless underground sensor networks," in *Proc. IEEE INFOCOM*, Mar. 2012, pp. 370–378.
- [19] S. Kisseleff, W. Gerstacker, R. Schober, Z. Sun, and I. F. Akyildiz, "Channel capacity of magnetic induction based wireless underground sensor networks under practical constraints," in *Proc. IEEE WCNC*, Apr. 2013, pp. 2603–2608.
- [20] T. Svantesson, M. A. Jensen, and J. W. Wallace, "Analysis of electromagnetic field polarizations in multiantenna systems," *IEEE Trans. Wireless Commun.*, vol. 3, no. 2, pp. 641–646, Mar. 2004.
- [21] D. P. Stapor, "Optimal receive antenna polarization in the presence of interference and noise," *IEEE Trans. Antennas Propag.*, vol. 43, no. 5, pp. 473–477, May 1995.
- [22] B. T. Walkenhorst and T. G. Pratt, "Polarization-based interference mitigation for OFDM signals in channels with polarization mode dispersion," in *Proc. IEEE MILCOM*, Nov. 2008, pp. 1–5.

- [23] H. Jiang and Y. Wang, "Capacity performance of an inductively coupled near field communication system," in *Proc. IEEE Int. Symp. Antenna Propag. Soc.*, Jul. 2008, pp. 1–4.
- [24] F. Sivrikaya and B. Yener, "Time synchronization in sensor networks: A survey," *IEEE Netw.*, vol. 18, no. 4, pp. 45–50, Jul. 2004.
- [25] H.-W. Beckmann *et al.*, *Friedrich Tabellenbuch Elektrotechnik/Elektronik*. Bonn, Germany: Ferd. Dümmlers Verlag, 1998, pp. 553–579, Auflage.
- [26] H. Lindner, H. Brauer, and C. Lehmann, *Taschenbuch der Elektrotechnik und Elektronik*. Leipzig, Germany: Fachbuchverlag, 2004, p. 8, Auflage.
- [27] Z. Sun, I. F. Akyildiz, S. Kisseleff, and W. Gerstacker, "Increasing the capacity of magnetic induction communications in RF-challenged environments," *IEEE Trans. Commun.*, vol. 61, no. 9, pp. 3943–3952, Sep. 2013.
- [28] E. E. Kriezis, T. D. Tsioukas, S. M. Panas, and J. A. Tegopoulos, "Eddy currents: Theory and applications," *Proc. IEEE*, vol. 80, no. 10, pp. 1559–1589, Oct. 1992.
- [29] C. Jordan and K. G. Balmain, *Electromagnetic Waves and Radiation Systems*, 2nd ed. Englewood Cliffs, NJ, USA: Prentice-Hall, 1968.
- [30] D. Tse and P. Viswanath, *Fundamentals of Wireless Communication*. Cambridge, U.K.: Cambridge Univ. Press, 2005.
- [31] Y. Zhang, Z. Zhao, and K. Chen, "Frequency splitting analysis of magnetically-coupled resonant wireless power transfer," in *Proc. IEEE ECCE*, Sep. 2013, pp. 2227–2232.
- [32] T.-Y. Feng, "A survey of interconnection networks," *Computer*, vol. 14, no. 12, pp. 12–27, Dec. 1981.
- [33] S. Boyd and L. Vandenberghe, *Convex Optimization*. Cambridge, U.K.: Cambridge Univ. Press, 2004.
- [34] R. C. Prim, "Shortest connection networks and some generalizations," *Bell Syst. Tech. J.*, vol. 36, no. 6, pp. 1389–1401, Jun. 1957.
- [35] W. Qin and Q. Cheng, "The constrained min-max spanning tree problem," in *Proc. ICIECS*, Dec. 2009, pp. 1–3.
- [36] M. Burkhart, P. von Rickenbach, R. Wattenhofer, and A. Zollinger, "Does topology control reduce interference?" in *Proc. MobiHoc*, 2004, pp. 9–19.



Steven Kisseleff (S'12) received the Dipl.-Ing. degree in information technology with focus on communication engineering from the University of Kaiserslautern, Kaiserslautern, Germany, in 2011. He is currently working toward the Ph.D. degree in electrical engineering with Friedrich-Alexander-University Erlangen-Nürnberg (FAU), Erlangen, Germany.

From 2010 to 2011, he was a Research Assistant with the Fraunhofer Institute of Optronics, System Technologies and Image Exploitation (IOSB). Since 2011, he has been a Research and Teaching Assistant with the Institute for Digital Communication, FAU. His research interests are in the area of digital communications, wireless sensor networks, and magnetic induction based transmissions.

Mr. Kisseleff was a recipient of Student Travel Grants for the IEEE Wireless Communications and Networking Conference 2013 and the IEEE International Conference on Communications 2014.



Ian F. Akyildiz (M'86–SM'89–F'96) received the B.S., M.S., and Ph.D. degrees from the University of Erlangen-Nürnberg, Erlangen, Germany, in 1978, 1981, and 1984, respectively, all in computer engineering. He is currently the Ken Byers Chair Professor in Telecommunications with the School of Electrical and Computer Engineering, Georgia Institute of Technology, Atlanta (Georgia Tech), GA, USA, and the Director of the Broadband Wireless Networking Laboratory and Chair of the Telecommunication Group at Georgia Tech.

He is an Honorary Professor with the School of Electrical Engineering, Universitat Politècnica de Catalunya, Barcelona, Spain, and founded the NaNoNetworking Center in Catalunya (N3Cat). Since September 2012, he has also been a FiDiPro Professor (Finland Distinguished Professor Program (FiDiPro) supported by the Academy of Finland) at the Department of Communications Engineering, Tampere University of Technology, Tampere, Finland. His current research interests are in wireless underground sensor networks, nanonetworks, and Long Term Evolution-Advanced networks.

Dr. Akyildiz is an ACM Fellow (1997). He is the Editor-in-Chief of *Computer Networks* (Elsevier) and the Founding Editor-in-Chief of *Ad Hoc Networks* (Elsevier), *Physical Communication* (Elsevier), and *Nano Communication Networks* (Elsevier). According to Google Scholar as of October 2014, his h-index is 83 and the total number of citations he received is 64211. He was a recipient of numerous awards from IEEE and ACM.



Wolfgang H. Gerstacker (S'93–M'98–SM'11) received the Dipl.-Ing. in electrical engineering and Dr.-Ing. and Habilitation degrees from the University of Erlangen-Nürnberg, Erlangen, Germany, in 1991, 1998, and 2004, respectively. Since 2002, he has been with the Chair of Mobile Communications (now renamed to Institute for Digital Communications) of the University of Erlangen-Nürnberg, currently as a Professor.

His research interests are in the broad area of digital communications and statistical signal processing.

Prof. Gerstacker has served as a Technical Program Committee Member of various conferences. He has been a Technical Program Co-Chair for the IEEE International Black Sea Conference on Communications and Networking (BlackSeaCom) 2014 and a Co-Chair for the Cooperative Communications, Distributed MIMO and Relaying Track of VTC2013-Fall. He has been an Editor of the IEEE TRANSACTIONS ON WIRELESS COMMUNICATIONS since 2012. Furthermore, he is an Area Editor of Elsevier's *Physical Communication* (PHYCOM) and has served as a Lead Guest Editor of a PHYCOM Special Issue on "Broadband Single-Carrier Transmission Techniques" (2013). He was a Member of the Editorial Board of *EURASIP Journal on Wireless Communications and Networking* from 2004 to 2012. He was a recipient of several awards, including the IEEE COM Innovation Award (2003), the Vodafone Innovation Award (2004), and the "Mobile Satellite & Positioning" Track Paper Award of VTC2011-Spring.